J. Fluid Mech. (1989), *vol.* 200, *pp.* 1–18
Printed in Great Britain

An iterative method for high-Reynolds-number flows with closed streamlines

By A. J. MESTEL

Department of Applied Mathematics and Theoretical Physics, University of Cambridge, Silver St., Cambridge CB3 9EW, UK

(Received 31 July 1987 and in revised form 31 August 1988)

In steady, two-dimensional, inviscid flows it is well-known that, in the absence of rotational forcing, the vorticity is constant along streamlines. In a bounded domain the streamlines are necessarily closed. In some circumstances, investigated in this paper, this behaviour is exhbited also by forced viscous flows, when the variation of vorticity across the streamlines is determined by a balance between viscous diffusion and the forcing. Similar results hold in axisymmetry. For such flows, an iterative process for finding the vorticity as a function of the stream function is described. The method applies whenever the viscous boundary condition can be expressed in terms of the vorticity or tangential stress rather then the tangential velocity. When it is applicable, the iterative method is faster than direct solution of the Navier–Stokes equations at high Reynolds numbers. As an example, the method is used to calculate the flow in a model of the electromagnetic stirring process. In this model, a conducting fluid in an elliptical region is driven by a rotating magnetic field and resisted by a surface stress. The functional dependence of the vorticity on the stream function is found for various values of the magnetic skin depth, surface stress and eccentricity of the ellipse. The form of the flow is discussed with particular reference to whether it consists of a single circulatory region or separates into two or more such regions.

1. Introduction

In classical hydrodynamics fluid motion in a closed container can only be driven by prescribing a velocity or stress along the boundaries. Vorticity generated at the walls spreads into the interior in a manner totally under the control of the fluid. When a rotational body force acts, however, vorticity may be generated in the main body of the fluid, widening considerably the range of achievable flows. In this paper we investigate a particular class of these flows.

We consider incompressible flow of a Newtonian fluid in a closed domain V bounded by a surface S under the influence of a prescribed rotational force field $\boldsymbol{F}(\boldsymbol{x})$. This force, which must be independent of the flow, may occur, for example, in low-Prandtl-number convection, when it is the buoyancy force due to a completely diffused temperature distribution (e.g. Busse & Clever 1981). Other examples include certain ocean models where a source of vorticity is prescribed (Read, Rhines & White 1986), and many magnetohydrodynamic flows of conducting fluids at low magnetic Reynolds number. In this latter case, an example of which we consider in §5, $\boldsymbol{F}$ is the Lorentz force per unit mass

$$\boldsymbol{F} = \frac{1}{\mu_0 \rho}(\nabla \wedge \boldsymbol{B}) \wedge \boldsymbol{B}, \tag{1.1}$$

where $\boldsymbol{B}$ is the magnetic field in the fluid, μ_0 the permeability and ρ the fluid density. This force is independent of the flow velocity $\boldsymbol{u}$ provided the induced e.m.f. due to the fluid motion, $\boldsymbol{u} \wedge \boldsymbol{B}$, is negligible.

The flow is governed by the Navier–Stokes equations

$$\nabla \cdot \boldsymbol{u} = 0, \tag{1.2}$$

$$\frac{\partial \boldsymbol{u}}{\partial t} + \nabla\left(\frac{p}{\rho} + \tfrac{1}{2}u^2\right) = \boldsymbol{u} \wedge \boldsymbol{\omega} + \boldsymbol{F} + \nu \nabla^2 \boldsymbol{u}, \tag{1.3}$$

and associated vorticity equation

$$\frac{\partial \boldsymbol{\omega}}{\partial t} = \nabla \wedge (\boldsymbol{u} \wedge \boldsymbol{\omega}) + \boldsymbol{G} + \nu \nabla^2 \boldsymbol{\omega}. \tag{1.4}$$

In the above $\boldsymbol{u}, \boldsymbol{\omega}, p, \rho$ and ν are respectively the velocity, vorticity, pressure, density and kinematic viscosity of the fluid, while $\boldsymbol{G} = \nabla \wedge \boldsymbol{F}$ is the source of vorticity due to the forcing. We shall suppose the flow to be such that the streamlines are closed. If we integrate (1.3) around a closed curve C which corresponds at time $t = t_0$ to one such streamline, we obtain

$$\frac{\partial}{\partial t}\left(\oint_C \boldsymbol{u} \cdot \mathrm{d}\boldsymbol{l}\right)_{|\, t = t_0} = \oint_C (\boldsymbol{F} + \nu \nabla^2 \boldsymbol{u}) \cdot \mathrm{d}\boldsymbol{l}, \tag{1.5}$$

implying that the circulation around any streamline adjusts itself until a balance is reached between the forcing and the viscous drag. Let us now consider steady solutions at high Reynolds number. Formally, we set $\partial/\partial t = 0$ and then let $\nu \to 0$. For ν large enough, we know from the general theory of the Navier–Stokes equations that a unique, stable steady solution will exist. As $\nu \to 0$, we shall assume that at least one steady solution continues to exist, though it may well lose its uniqueness and its stability. In this introduction we discuss the possible asymptotic forms of such a solution. We distinguish the following possibilities:

(*a*) The velocity $\boldsymbol{u}$ may scale as $1/\nu$.

(*b*) The streamlines may align themselves so that $\oint \boldsymbol{F} \cdot \mathrm{d}\boldsymbol{l} = 0$ on every streamline.

(*c*) The lengths of the streamlines may increase without limit as $1/\nu$.

(*d*) Every streamline may pass through a singular region based on a small lengthscale such as a viscous boundary layer.

(*e*) The flow may divide into two or more regions each governed by one of (*a*)–(*d*).

In this paper we shall be concerning ourselves mainly with case (*a*). When (*a*) holds, the forcing and viscous terms are locally of the same order of magnitude, while the inertial term is greater than either. A severe limitation on the applicability of case (*a*) is that the scaling $\boldsymbol{u} \sim 1/\nu$ does not permit the existence of a dissipative boundary layer of the sort normally associated with solid boundaries. For with this scaling, the rate of energy dissipation in the main body of the fluid is of the same order as the rate of working of the driving force. Thus the dissipation in any boundary layer cannot exceed that of the main flow.

Case (*b*) is very special in that it permits the existence of a steady inviscid solution, with the forcing and inertia terms everywhere balancing. Such flows are very uncommon. Frequently, we can infer from the form of $\boldsymbol{F}$ and $\boldsymbol{G}$ that such a balance is impossible. Clearly, unless $\oint \boldsymbol{F} \cdot \mathrm{d}\boldsymbol{l} = 0$ along a surface streamline, a condition not often satisfied in practice, case (*b*) is excluded. A further necessary condition for case

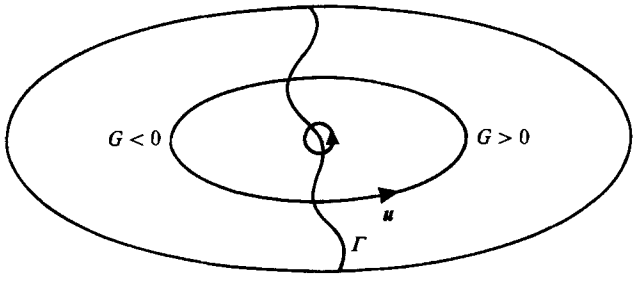

FIGURE 1. Distribution of G for a possible inviscid solution as in case (*b*).

(*b*) to occur in two-dimensional flow is that there should exist a curve, Γ, on which $G = |\boldsymbol{G}| = 0$ and which divides the region of flow into two as in figure 1. The centre of circulation could then lie on this curve. These conditions are not sufficient, however, and in general flows driven by such functions G will split into two or more counter-circulating viscous regions (as, for example, does flow in a circular cylinder driven by an alternating, uniform magnetic field). Should circumstances be such that a flow of type (*b*) exists, then it will not be uniquely defined if the viscous terms are totally neglected. (Trivially, the transformation $\boldsymbol{u} \rightarrow -\boldsymbol{u}$ would then also define a solution, and there would be other degeneracies.) Subsidiary conditions obtained from the $O(\nu)$ corrections to the leading-order flow would be needed for uniqueness. Despite its rarity of occurrence, case (*b*) is the only one of the above cases that permits a steady asymptotic solution in which the velocity remains bounded. It is thus of interest when the shape of the boundary S is determined by a balance of normal stress, and is thus unable to support the dynamic pressures associated with large variations in the velocity. Such circumstances hold in the levitation melting process (Mestel 1982; Sneyd & Moffatt 1982).

Case (*c*) is of particular interest when the flow under consideration is two-dimensional and unbounded in the third dimension. Davidson & Hunt (1987) describe how weak three-dimensionality in the driving force $\boldsymbol{F}$ can lead to secondary flows in the third-dimension on a lengthscale $1/\nu$, thus explaining observed deep three-dimensional motions in the continuous casting process in steel manufacture. When the domain is bounded in the third dimension also, however, these deep motions pass through a boundary layer on the walls as in case (*d*). For case (*c*) to apply in a bounded domain, it is clear that as $\nu \rightarrow 0$ each streamline must develop a structure based on a small lengthscale. In three dimensions one cannot rule out the possibility of velocity variations on this lengthscale (as in case *d*), but this is unlikely since G is independent of ν. A more common structure would have gradually spiralling streamlines similar to those of an $O(1)$ poloidal flow superposed on an $O(\nu)$ toroidal flow. Such flows can be represented by a flow whose streamlines close on the large lengthscale, with a small correction due to the sideways drift.

A full analysis of the kind of boundary layer required in case (*d*) has yet to be done, although it is a very important case in practice. Most two-dimensional flows driven by a rotational force in a solid container will develop such a structure. There seems to be some evidence that the boundary-layer thickness scales as $\nu^{\frac{1}{3}}$, with a jet-like velocity proportional to $\nu^{-\frac{1}{3}}$ (Fautrelle 1981; Mestel 1984; Sneyd 1979). Sneyd argues that such a boundary layer is likely to be unstable to perturbations akin to Taylor vortices, but it would nevertheless be of interest to understand the asymptotic behaviour. Many magnetohydrodynamic flows of this kind are in reality turbulent, but may be modelled reasonably well by steady, laminar solutions.

As for case (*e*), it should be noted that each of the cases (*a*)–(*d*) involves a different scaling for the velocity and its scale of variation. Thus it would require some fairly delicate asymptotic matching for two such cases to exist simultaneously. Case (*a*), for example, can only coexist with another case if the velocity vanishes on the boundary of the region where (*a*) holds.

Whichever of the above cases applies, the forcing and dissipation balance according to the streamline integrals

$$\oint (\boldsymbol{F} + \nu \nabla^2 \boldsymbol{u}) \cdot \mathrm{d}\boldsymbol{l} = 0. \tag{1.6}$$

Physically, because the flow is steady and the streamlines are closed, the viscous term acts over a very long time and no matter how small it is, it must be balanced by the forcing. In case (*a*), with which we shall be concerned from now on, inertial forces are locally dominant, and (1.4) reduces to

$$\nabla \wedge (\boldsymbol{u} \wedge \boldsymbol{\omega}) = 0. \tag{1.7}$$

Equations (1.6) and (1.7), together with a suitable boundary condition on S, define the flow to lowest order in ν. In the next section we shall apply (1.6) and (1.7) to geometrically simple flows that are either two-dimensional or axisymmetric and poloidal. In these cases we can derive an integro–differential equation for the vorticity which we aim to solve iteratively. In §3 we discuss the possible boundary conditions on S consistent with this formation. In §4 we describe the mechanics of the iterative process and the numerical alogorithms used. In §§5 and 6 we apply the method to the particular problem of rotating magnetic field around a conducting, elliptical cylinder. We conclude in §7.

2. Two-dimensional and axisymmetric flows

When the flow is either two-dimensional or axisymmetric and poloidal (without swirl) then for topological reasons the streamlines must be closed and (1.6) applies. We shall first consider the two-dimensional case. If we introduce a stream function ψ, where $\boldsymbol{u} = \nabla \wedge (0, 0, \psi(x, y))$ in terms of Cartesian coordinates, then (1.7) reduces to

$$\boldsymbol{u} \cdot \nabla \omega = 0, \tag{2.1}$$

where ω is the magnitude of the vorticity $\boldsymbol{\omega}$, implying a functional relation between ω and ψ

$$\omega = \omega(\psi). \tag{2.2}$$

Thus
$$\nabla^2 \boldsymbol{u} = -\nabla \wedge \boldsymbol{\omega} = -\frac{\mathrm{d}\omega}{\mathrm{d}\psi} \boldsymbol{u} \tag{2.3}$$

and so (1.6) may be written

$$\frac{\mathrm{d}\omega}{\mathrm{d}\psi} = \frac{\oint \boldsymbol{F} \cdot \mathrm{d}\boldsymbol{l}}{\nu \oint \boldsymbol{u} \cdot \mathrm{d}\boldsymbol{l}} = \frac{\int_A G \mathrm{d}A}{\nu \int_A \omega \, \mathrm{d}A}, \tag{2.4}$$

where $A(\psi)$ is the area enclosed by the streamline $\psi =$ constant, and $G = |\boldsymbol{G}|$. This relation, together with

$$\omega = -\nabla^2 \psi \quad \text{in} \quad V; \qquad \psi = 0 \quad \text{on} \quad S \tag{2.5}$$

and a suitable further boundary condition (e.g. ω given on S) suffices to define the flow. Equation (2.4) has been given by many authors (e.g. Read *et al.* 1986). It has

a physical interpretation that the rate of increase of vorticity across a streamline is the ratio of the total source of vorticity to the total vorticity inside that streamline. In a companion paper (Mestel 1989) we found that instability is likely to occur when $\mathrm{d}\omega/\mathrm{d}\psi$ is large and positive, which we can interpret as an inadequate production of vorticity for a given strength of source.

Similar results hold for poloidal axisymmetric flows. Equation (1.7) implies

$$\frac{\omega}{r} = \Omega(\psi) \tag{2.6}$$

for some function Ω, where $\psi(r, z)$ is now the Stokes stream function, so that $\boldsymbol{u} = \boldsymbol{\nabla} \wedge (0, \psi/r, 0)$ in terms of cylindrical coordinates (r, θ, z). Then, following Jones, Moore & Weiss (1976), we have

$$\nabla^2 \boldsymbol{u} = -\boldsymbol{\nabla} \wedge \boldsymbol{\omega} = -r^2 \frac{\mathrm{d}\Omega}{\mathrm{d}\psi} \boldsymbol{u} - 2\Omega \hat{\boldsymbol{z}}, \tag{2.7}$$

where $\hat{\boldsymbol{z}}$ is a unit vector in the z-direction. Now the last term in (2.7) is constant along a streamline and thus

$$\oint \nabla^2 \boldsymbol{u} \cdot \mathrm{d}\boldsymbol{l} = -\frac{\mathrm{d}\Omega}{\mathrm{d}\psi} \oint r^2 \boldsymbol{u} \cdot \mathrm{d}\boldsymbol{l} \tag{2.8}$$

and so (1.6) implies

$$\frac{\mathrm{d}\Omega}{\mathrm{d}\psi} = \frac{\oint \boldsymbol{F} \cdot \mathrm{d}\boldsymbol{l}}{\nu \oint r^2 \boldsymbol{u} \cdot \mathrm{d}\boldsymbol{l}} = \frac{\int_A G \, \mathrm{d}A}{\nu \int_A r^3 \Omega \, \mathrm{d}A} \tag{2.9}$$

since $\int_A \partial\psi/\partial r \, \mathrm{d}A = 0$. Once again (2.9), together with

$$\mathrm{D}^2 \psi = -r^2 \Omega(\psi) \quad \text{in} \quad V; \qquad \psi = 0 \quad \text{on} \quad S \tag{2.10}$$

where D^2 is the Stokes operator,

$$\mathrm{D}^2 = r \frac{\partial}{\partial r} \frac{1}{r} \frac{\partial}{\partial r} + \frac{\partial^2}{\partial z^2}, \tag{2.11}$$

define the flow subject to a suitable boundary condition on S.

Batchelor's (1956) results, that ω and Ω are constant if $\boldsymbol{F}$ vanishes (or is conservative), follow directly from (2.4) and (2.9). However when $G \neq 0$ these equations cannot be solved simply, as their right-hand sides depend on ω and Ω in a complex manner. Nevertheless, we can envisage an iterative solution. If we regard ψ as a known function of position then these right-hand sides involve integrals of known functions along known curves and can therefore be evaluated for each value of ψ. Equation (2.4) or (2.9) can then be integrated, subject to a suitable boundary condition, to find the vorticity distribution. The Poisson equation (2.5) or (2.10) can then be solved for this vorticity to find a new stream function and the process repeated. As each stage in this iteration involves integration we might expect it to converge. This method is discussed in detail in §4, but first we discuss the form of the required boundary condition.

3. The boundary condition

It is clear from the above sketch of a method of solution of (2.4) and (2.5) or the analagous (2.9) and (2.10) that we require a boundary condition for ω (or Ω) on S. The simplest such condition, that ω should be constant on S, is uncommon physically. Normally we would expect either the velocity to be prescribed on S or that the normal velocity and the tangential stress should be given. We might very well expect

there to be a connection between the cases when either the surface vorticity or the tangential stress is prescribed, and we show below that this is indeed the case. First, however, we consider when a no-slip boundary gives an appropriate condition.

If the velocity on S is prescribed, then we can use the relation

$$\int_V \omega \, \mathrm{d}A = \oint_S \boldsymbol{u} \cdot \mathrm{d}\boldsymbol{l} \tag{3.1}$$

as the required boundary condition for the iterative process. For if ψ is regarded as a known function of position, then integrating (2.4) and substituting into (3.1) defines the requisite constant value, ω_0, of the vorticity on S. However, this does not, in general, give the required solution. Instead of a flow satisfying a no-slip condition on S, we shall obtain one that separates into two or more circulatory regions with oppositely signed vorticity, so that the total vorticity in V is zero. As we discussed in §1, for flows with a solid boundary, the scaling $\boldsymbol{u} \sim 1/v$ is usually inappropriate. Instead, the streamlines pass through a boundary layer in order to ensure the balance (1.6) as in case (*d*) of §1. However, there are special cases when a solution of this type does exist, when (3.1) will define a solution for a no-slip boundary. One such case is that of two-dimensional circular flow. When S is circular, then provided the force $\boldsymbol{F}(r,\theta)$ is such that its average with respect to θ does not vanish identically for every r, (1.6) and (1.7) will define a flow with circular streamlines. Because of its θ-independence, the velocity can vanish simultaneously everywhere on S. Should the force $\boldsymbol{F}$ itself be independent of θ, then the circular flow will be a solution to the full Navier–Stokes equations. This case has been much studied as a model of electromagnetic stirring in the metallurgical industry (e.g. Moffatt 1965; Davidson & Hunt 1987). For non-circular shapes S, only special force distributions $\boldsymbol{F}$ will give rise to a solution without a boundary layer as we require. It should be noted that these exceptional flows are much more energetic than those where the boundary offers severe resistance to the inertially dominated core flow.

We have already observed in §1 and above that the scaling $\boldsymbol{u} \sim 1/v$ does not permit a dissipative boundary layer such as we would normally expect on a solid surface. However, there is no such objection to a weak boundary layer across which the velocity is continuous but the tangential stress changes. Such a boundary layer may be linearized and solved in terms of the surface velocity and coordinates local to S (e.g. Batchelor 1967). Thus in the two-dimensional case for example, if n and s are coordinates respectively normal and tangential to S, then the boundary-layer equation for $\omega(n,s)$

$$u_n \frac{\partial \omega}{\partial n} + u_s \frac{\partial \omega}{\partial s} = \nu \frac{\partial^2 \omega}{\partial n^2} \tag{3.2}$$

reduces to Von Mise's equation

$$\frac{\partial \omega}{\partial s} = \nu U(s) \frac{\partial^2 \omega}{\partial \psi^2} \tag{3.3}$$

for $\omega(\psi, s)$, where $U(s)$ is the surface velocity and $\psi = nU(s)$. The relation between vorticity and tangential stress per unit density, τ, is

$$\tau = \nu[\omega - 2K(s)U], \tag{3.4}$$

where K is the curvature of S, and so the boundary conditions for (3.3) are

$$\begin{aligned} &\omega = \tau/\nu + 2KU \quad \text{on} \quad \psi = 0, \\ &\omega \to \omega_0 \qquad\quad \text{as} \quad \psi/\nu^{\frac{1}{2}} \to \infty, \end{aligned} \tag{3.5}$$

where ω_0 is the appropriate (constant) value of the vorticity as the boundary layer matches onto the core flow. Now for the streamlines to be closed, ω, must be periodic in s, and so from (3.3)

$$\frac{\partial^2}{\partial \psi^2} \oint U\omega \, ds = 0. \tag{3.6}$$

Integrating (3.6) subject to (3.5) then gives

$$\omega_0 = \frac{\oint_S (2KU + \tau/\nu) U \, ds}{\oint_S U \, ds}. \tag{3.7}$$

We have thus derived a boundary condition which we can use for the core flow defined by (2.4) and (2.5).

We could also have derived (3.7) from considerations of energy balance. Integrating the scalar product of (1.3) with $\boldsymbol{u}$ we obtain the energy equation

$$\int_S \boldsymbol{u}\cdot\boldsymbol{\tau} \, dS + \int_V \boldsymbol{u}\cdot\boldsymbol{F} \, dV = 2\nu \int_V e_{ij} e_{ij} \, dV, \tag{3.8}$$

where $e_{ij} = \frac{1}{2}(\partial u_i/\partial x_j + \partial u_j/\partial x_i)$ is the rate-of-strain tensor. Now we know that the energy dissipation within the boundary is negligible. Equation (3.8) should therefore apply whether the surface S is taken to be inside or outside the boundary layer. Thus $\int \boldsymbol{u}\cdot\boldsymbol{\tau} \, dS$ does not vary across the boundary layer and (3.7) follows.

Equation (3.7) defines an equivalent constant surface vorticity for any given stress distribution. With regard to our planned iterative approach we can see that a given velocity distribution at once defines a surface vorticity which will eventually produce a new velocity distribution. For this iteration process to converge for any inital estimate of ω_0, it is clear that we must require

$$\oint 2Ku_0^2 \, ds < \oint u_0 \, ds, \tag{3.9}$$

where u_0 is the surface velocity due to unit vorticity in V. (Otherwise an initially large estimate will grow larger.) The relation (3.9) is violated only when S is circular when equality holds. A moment's reflection reveals that this is only to be expected, as the problem is ill-posed in that case. Physically, the force $\boldsymbol{F}$ is providing a torque on the (circular) region V which will therefore spin up without limit unless the tangential stress τ exactly balances it. The difference between the circular case and all others is that no distribution of *normal* stress on S can affect the balance of moments about the centre of the circle. For all other shapes, an appropriate normal stress guarantees global equilibrium and the existence of a solution. In the next section we describe in more detail the iterative method that calculates the flow whenever ω or τ is given on S.

4. The iteration procedure

We shall concentrate on the two-dimensional case in this section, commenting on the differences with axisymmetric flows towards the end.

The equations to be solved are

$$\omega = -\nabla^2\psi \quad \text{in} \quad V; \qquad \psi = 0 \quad \text{on} \quad S, \tag{4.1}$$

$$\frac{d\omega}{d\psi} = \frac{\oint \boldsymbol{F}\cdot d\boldsymbol{l}}{\nu \oint \boldsymbol{u}\cdot d\boldsymbol{l}} = \frac{\int G \, dA}{\nu \int \omega \, dA}, \tag{4.2}$$

$$\omega = B[\omega] \quad \text{on} \quad S, \tag{4.3}$$

where B denotes some boundary condition which is in some sense attractive, so that repeated applications of (4.3) will converge. Normally B will either be a constant or the stress condition (3.7).

We aim to use the method for an arbitrary domain V, and must decide how best to solve the Poisson equation (4.1) and to calculate the streamline integrals in (4.2). In fact it is convenient to exploit the two-dimensionality of the problem by using conformal transformations, although this is not an essential part of the method. If we transform from the region V in the Z-plane to the unit disc in the Z'-plane ($Z = x+\mathrm{i}y$, $Z' = x'+\mathrm{i}y'$), then the Laplacian transforms according to

$$\nabla^2 \to \frac{1}{J}\nabla'^2, \tag{4.4}$$

where the Jacobian

$$J = \frac{\partial(x, y)}{\partial(x', y')} = \left|\frac{\mathrm{d}Z}{\mathrm{d}Z'}\right|^2. \tag{4.5}$$

Thus (4.1) transforms into

$$\nabla'^2\psi = -J(r', \theta')\,\omega \quad \text{in} \quad r' < 1; \qquad \psi = 0 \quad \text{on} \quad r' = 1, \tag{4.6}$$

where r', θ' are polar coordinates, while (4.2) becomes

$$\frac{\mathrm{d}\omega}{\mathrm{d}\psi} = \frac{\int JG\,\mathrm{d}A'}{\nu\int J\omega\,\mathrm{d}A'} = \frac{\oint \boldsymbol{F}'\cdot\mathrm{d}\boldsymbol{l}'}{\nu\oint \boldsymbol{u}'\cdot\mathrm{d}\boldsymbol{l}'}. \tag{4.7}$$

The boundary condition (4.3) also transforms accordingly. We shall suppress the primes on the variables in what follows without ambiguity. This method of conformal transformation is often used in two-dimensional Navier–Stokes calculations as it leaves the vorticity equation unchanged in the absence of rotational forces (e.g. Tutty & Pedley 1989). It has the practical advantage that one can write a single routine using an accurate centred-difference scheme for which one need supply only the curl of the forcing, G, and the Jacobian, J. This outweighs the disadvantage of having to find an appropriate conformal mapping whose Jacobian may vary appreciably over V. For our problem the method has an additional advantage in that it facilitates the solution of the Poisson equation (4.1). We can derive the Green function for (4.6)

$$H(x,x_0) = \frac{1}{4\pi}\log\left[\frac{r^2+r_0^2-2rr_0\cos(\theta-\theta_0)}{1+r^2r_0^2-2rr_0\cos(\theta-\theta_0)}\right] \tag{4.8}$$

satisfying

$$\nabla^2 H = \delta(x-x_0) \quad \text{in} \quad r < 1, \qquad H = 0 \quad \text{on} \quad r = 1 \tag{4.9}$$

so that

$$\psi(\boldsymbol{x}) = \int_{r_0<1} H(\boldsymbol{x}, \boldsymbol{x}_0)\, J(\boldsymbol{x}_0)\, \omega(\boldsymbol{x}_0)\,\mathrm{d}A_0. \tag{4.10}$$

We define a regular polar gird in the unit disc

$$r = \frac{m}{N_r}, \quad \theta = 2\pi\frac{n}{N_\theta}, \quad 0 \leqslant n \leqslant N_r, \quad 0 \leqslant n \leqslant N_\theta. \tag{4.11}$$

We approximate the integral in (4.10) using the trapezium rule, except close to the singularity of the Green function where we perform the integration analytically to the same order. This defines a matrix $\boldsymbol{M}$, dependent solely on the geometry, such that

$$\psi_{ij} = M_{ijkl}\,\omega_{kl} \tag{4.12}$$

where the suffices to ψ and ω denote values at the appropriate grid points. Starting from a vorticity distribution ω_{kl}, we choose a suitable number (N_ψ) of values $\psi^{(n)}$ between the minimum and maximum values of ψ. Next we calculate the (r, θ)-coordinates of the intersections of the streamlines $\psi = \psi^{(n)}$ with the grid lines (as would a graphical contouring routine). The streamline integrals along these contours are then calculated and the new values $\omega(\psi^{(n)})$ found by Runge–Kutte integration of (4.7) with (4.3). The new vorticity distribution on the grid $\omega_{kl} = \omega(\psi_{kl})$ is found by spline interpolation of these values. Finally, the new vorticity is tested for convergence and if necessary another iteration is performed.

All that remains is to find G and J for the problem under consideration. Very often an explicit conformal mapping will be available for idealized problems, such as the one we consider in §§5 and 6. If necessary, the transformation may be calculated numerically (Trefethen 1986). The scheme is second order in the steplengths, although some care should be taken near points where the Jacobian is large for maximum accuracy.

A similar scheme can be used for axisymmetric problems. The main difference is that the conformal-mapping techniques are not available. Thus it is necessary to supply a suitable grid for a given problem and some other method must be used to solve the Poisson-like equation (2.10). One such method would be to use relaxation on the supplied grid (e.g. Mestel 1982). Otherwise the strategy for axisymmetric problems is the same as for two-dimensional ones.

The method converges very rapidly, six iterations usually sufficing even for fine grids. It is noticeably faster than high-Reynolds-number Navier–Stokes calculations, although the latter are of course more versatile. The program was tested for accuracy against one of these, very kindly supplied and modified by Dr Tutty. His program solves the Navier–Stokes equations in a square, and so for comparison it was necessary to map the unit disc in the Z'-plane onto the square in the Z''-plane, using the transformation

$$Z' = \frac{1}{\sqrt{2}} sd\,(K[\tfrac{1}{2}]\,Z''\,|\,\tfrac{1}{2}), \tag{4.13}$$

where sd is an elliptic function and $K[m]$ is the complete elliptic integral (Abramowitz & Stegun 1965). The comparison showed that the above scheme is indeed second order and was very useful as a debugging aid. The numerical results for the particular case discussed in the following section are presented in §6.

5. Rotating magnetic field around a conducting ellipse

We have already observed that a circular boundary gives rise to a singular case in which the inertial forces are exactly balanced by radial pressure gradients, and the form of the solution is the same for all Reynolds numbers. Sneyd (1979) calculated the perturbation to the flow when a no-slip circular boundary is perturbed slightly, and showed that that perturbation is indeed singular at high Reynolds number. For slippery boundaries, however, the effect of non-circularity is not as great. A natural generalization is to consider an elliptical boundary S

$$\frac{x^2}{a^2} + \frac{y^2}{b^2} = 1 \tag{5.1}$$

parametrized by $(x, y) = (a \cos\theta, b \sin\theta)$. Such a shape covers the spectrum between the almost circular ($a \approx b$) and the almost one-dimensional ($a \gg b$). We shall use a non-dimensional lengthscale such that $ab = 1$.

We have seen that we shall require a conformal transformation for the interior of S onto the unit disc in the Z'-frame. Such a mapping is defined by

$$Z = (a^2 - b^2)^{\frac{1}{2}} \cosh \zeta \tag{5.2}$$

and

$$Z' = (1-m)^{\frac{1}{4}} nd(k\zeta|m), \tag{5.3}$$

where nd is an elliptic function whose parameter m and scale factor k are given by

$$K[m]k = 2\tanh^{-1}\left(\frac{b}{a}\right), \quad K[1-m]k = \tfrac{1}{2}\pi, \tag{5.4}$$

where $K[m]$ once again is the complete elliptic integral (Abramowitz & Stegun 1965). The above transformation should not be confused with the more commonly known (5.16) which maps onto the *exterior* of the unit disc. Equation (5.2) may be used to define elliptic coordinates μ and θ, where $\zeta = \mu + i\theta$, so that

$$x = (a^2 - b^2)^{\frac{1}{2}} \cosh\mu \cos\theta, \quad y = (a^2 - b^2)^{\frac{1}{2}} \sinh\mu \sin\theta. \tag{5.5}$$

We consider now a problem of relevance to the continuous casting process for the manufacture of metals, wherein a gradually solidifying column of liquid metal is stirred by a rotating magnetic field. Analytical work on this probelm has assumed a circular cross-section, but such is rarely the case in practice. In general, a numerical approach is required and in some circumstances the method described in §4 can be used. During solidification of such a column, a so-called 'mushy zone' forms around the solid–liquid interface. It has been suggested privately to the author that the effects of these dendritic regions on the interior circulating flow could be modelled using a resistive surface stress rather than a no-slip condition on the outer boundary. A suitable frictional relation would be

$$\tau = -\alpha \frac{\nu U}{L}, \tag{5.6}$$

where $U(s)$ is the surface velocity, L is an appropriate lengthscale and α is a dimensionless constant. For such a model, the method described in this paper is applicable, as we describe below.

A related metallurgical problem whose solution would be very similar occurs during electromagnetic shaping (Etay 1980; Shercliff 1981). Here, a suitable distribution of imposed alternating currents is used to distort the free surface of a liquid metal column into a desired shape. In such a process, the fluid motion must be taken into account, as this affects the surface pressure distribution for moderate field frequencies. Thus, if (say) an elliptical cross-section were desired, it would be essential to be able to calculate the flow in an ellipse in order to decide where to position the driving currents. The mathematics for fixed alternating fields is very similar to that for rotating fields, and so this problem could be solved in a very similar manner to that below. An important difference between the two cases is that for rotating fields, G is typically positive everywhere, whereas oscillating fields lead to forcing which has both positive and negative regions of G. Thus, the former tends to drive flows with a single circulatory region, while the latter tends to drive two or more counter-circulating regions.

The force on a conductor due to a rotating, initially uniform magnetic field requires some calculation, and in the remainder of this section we describe how it can

be found. If we let the field at infinity be $B_0(\cos ft, -\sin ft, 0)$ where f is the rotation frequency, and represent the magnetic field by

$$\boldsymbol{B} = \mathrm{Re}\,[\boldsymbol{\nabla} \wedge (0, 0, \chi e^{ift})], \tag{5.7}$$

where Re denotes the real part, then the flux function χ satisfies

$$\nabla^2\chi = \begin{cases} 0 & \text{outside } V \\ 2i\chi/\delta^2 & \text{inside } V. \end{cases} \tag{5.8}$$

Here the skin depth $\delta >$ is defined by

$$\delta = \left(\frac{2}{\mu_0 \sigma f}\right)^{\frac{1}{2}}, \tag{5.9}$$

where μ_0 is the permeability and σ the conductivity of the fluid. The boundary condition at infinity is then

$$\chi \sim -iB_0(x+iy). \tag{5.10}$$

The time-averaged curl of the Lorentz force per unit mass, $\boldsymbol{G}$, may be found from

$$\boldsymbol{G} = (0, 0, G) = \frac{1}{\delta^2 \mu_0 \rho}\mathrm{Im}\,[\boldsymbol{\nabla}\chi \wedge \boldsymbol{\nabla}\chi^*] \tag{5.11}$$

where Im denotes the imaginary part and * the complex conjugate.

Inside the elliptic domain V, (5.8) becomes, in terms of the elliptical coordinates of (5.5),

$$\frac{\partial^2\chi}{\partial\mu^2} + \frac{\partial^2\chi}{\partial\theta^2} = \begin{cases} 0 & \text{outside } V \\ (a^2-b^2)(\cosh 2\mu - \cos 2\theta)i\chi/\delta^2 & \text{inside } V, \end{cases} \tag{5.12}$$

and could be solved for any δ in terms of Mathieu functions, but these are somewhat cumbersome to use. Instead we find asymptotic solutions for δ small and large, which are sufficiently accurate to match up. For δ large (the low-frequency approximation) we find a series solution of (5.12) in powers of $1/\delta^2$. The leading-order term is just that due to a uniform rotating field

$$G = \frac{2B_0^2}{\mu_0 \delta^2 \rho} \tag{5.13}$$

and is constant over V (this holds for any region V). Higher-order terms may be found by straightforward perturbation methods applied to (5.12) and (5.10). We obtain the expansion

$$\chi = B_0 \sum_{k=0}^{\infty} \frac{1}{\delta^{2k}} \sum_{\substack{m,n=1 \\ \text{odd}}}^{2k+1} (A_{mnk} \cosh m\mu \cos n\theta + B_{mnk} \sinh m\mu \sin n\theta), \tag{5.14}$$

where the coefficients A_{mnk} and B_{mnk} are linear multiples of $A_{mn(k-1)}$ and $B_{mn(k-1)}$. This series is easily evaluated numerically giving accurate results for δ larger than about 0.5 (for $a/b < 2$). Below this value the series appears to diverge, although this may be a truncation effect. Padé approximant techniques increase the range of validity of the series down to $\delta \approx 0.2$, but below this value it is more sensible to use a high-frequency, or 'skin-depth' approximation.

For δ small, it is well known that the magnetic field is confined to a skin layer of

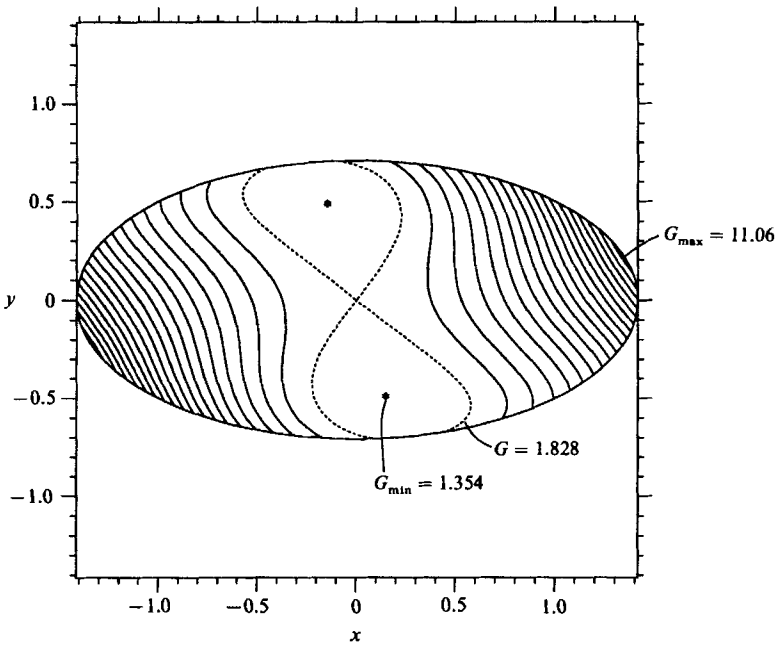

FIGURE 2. Equally spaced contours of G for a magnetic field rotating anticlockwise, $a/b = 2$, $\delta = 0.25$.

thickness δ near the surface S. In terms of the normal distance n from the surface S, parametrized by θ, it can be shown that inside V as $\delta \to 0$

$$\chi = \frac{\delta}{1+\mathrm{i}} B_s(\theta) \frac{\mathrm{e}^{-(1+\mathrm{i})n/\delta}}{(1-K(\theta)n)^{\frac{1}{2}}} + O(\delta^2), \tag{5.15}$$

where B_s is the tangential field that would result were the fluid a perfect conductor and excluded $\boldsymbol{B}$ totally, while K is the curvature of S. The result (5.15) has not been published before to the author's knowledge. Usually the less accurate approximation in which the square root in the denominator is omitted has been used (e.g. Mestel 1984). The derivation of (5.15) including the $O(\delta^2)$-term will be published elsewhere along with a description of the behaviour near the involute of S, where $n = 1/K$ (Mestel 1988).

The surface field B_s may be calculated by potential theory. The exterior of the ellipse may be mapped onto the *exterior* of the unit circle in the Z'-plane by

$$Z = \frac{a+b}{2} Z' + \frac{a-b}{2} \frac{1}{Z'}. \tag{5.16}$$

The solution is then found to be

$$B_s = \frac{B_0(a+b)\mathrm{e}^{\mathrm{i}\theta}}{(b^2\cos^2\theta + a^2\sin^2\theta)^{\frac{1}{2}}}. \tag{5.17}$$

We use (5.11), (5.17) and (5.15) (including the next-order term for greater accuracy) to provide an expression for G with a relative error of $O(\delta^2)$. This is sufficient to match onto the low-frequency estimate found from (5.14) with a manageable error.

Usually for flows of this type the form of G gives greater insight than does F, part of which is merely cancelled by the pressure gradient. Here we observe that G is always positive, is symmetric about the origin but is not symmetric about either of

the axes. The conductor resists the rotation of the field lines, leading to a concentration of gradient after the bulging major axes, as in figure 2. There, the contours of G are plotted for $\delta = 0.25$ and $a = 1/b = \sqrt{2}$ between its maximum of about 11 on the surface and its minimum of about 1.35 in the interior. This minimum occurs surprisingly close to the surface, with a saddle point at the centre of the ellipse. For δ large, G is small and uniform, as given by (5.13). It increases in magnitude as δ decreases through 1 past which it becomes localized in the skin layer. As $\delta \to 0$, it drives less and less circulation, the velocity $\boldsymbol{u}$ being proportional to δ. In this limit, the electromagnetic force as a surface stress (Mestel 1982; Moffatt 1984) as illustrated by the numerical results of the next section. In this context it is important to note that the two limits $\nu \to 0$ and $\delta \to 0$ may not be interchangeable, especially if dealing with solid boundaries.

6. Numerical results

The method outlined in §4 was used to solve the problem described in §5 using the transformation and forcing defined there. The velocity was non-dimensionalized so that effectively

$$\frac{B_0^2}{\mu_0 \rho} = 1. \tag{6.1}$$

Except for small values of the skin depth δ which require high resolution, the mesh sizes used were $N_r = 20$, $N_\theta = 96$, and $N_\psi = 20$. Solutions for ω and ψ were obtained for various values of δ, a/b, and the boundary condition on S. In figure 3, ω is drawn as a function of ψ for a stress-free ellipse with $a/b = 2$. Solutions are shown for various values of the skin depth δ, those on the right corresponding to δ large, while those on the left to δ small. When δ is large G is approximately constant, as given by (5.13), and both ω and ψ scale as $1/\delta^2$. As δ decreases, the net circulation increases (as measured by $\psi_{\max}$, the maximum value of ψ attained) reaching a maximum at about $\delta = 0.275$. The existence of this maximum is a common feature of electromagnetic stirring problems. As δ decreases, from this value, G becomes confined to the skin layer. Thus, fewer and fewer streamlines feel its effect, and the vorticity tends to a constant in the interior, but varies sharply over the skin layer. This constant, ω_c, can be calculated in terms of the tangential field B_s of (5.15) by considerations of energy balance (as in Mestel 1982 for the axisymmetric case). The straight dotted line on the left of figure 3 shows the asymptotic behaviour of $(\omega_c(\delta), \psi_{\max}(\delta))$ as $\delta \to 0$ which agrees well with the numerics.

Figure 4 shows a (ω, ψ)-plot for $a = 1/b = 1.1$ and $\delta = 0.1$, with ω taking a variety of values ω_0 on the boundary. As we discuss in the contiguous paper on stability (Mestel 1989), for ω_0 large and of either sign, the flow consists of a single circulatory region in the same sense as ω_0. The direction of circulation changes over a range of values of ω_0, the flow becoming unstable during this transition. A total flow reversal of the type shown to be unstable in that paper, would be represented in the figure by an infinite gradient of the curve $\omega = \omega(\psi)$, at the point corresponding to the streamline on which $\boldsymbol{u}$ vanishes. Should a curve $\omega = \omega(\psi)$ pass through regions of both positive and negative ψ, then the corresponding flow would have regions of both clockwise and anticlockwise circulation. For $\delta = 0.1$, the range of values of ω_0 over which the direction of circulation changes is fairly narrow ($-0.1 < \omega_0 < -0.25$). This is because the force $\boldsymbol{F}$ approximates to its asymptotic state of a tangential surface stress, when only values of ω_0 that correspond in (3.7) to an equal and opposite stress lead to irregular behaviour. (Otherwise the flow is simply being driven

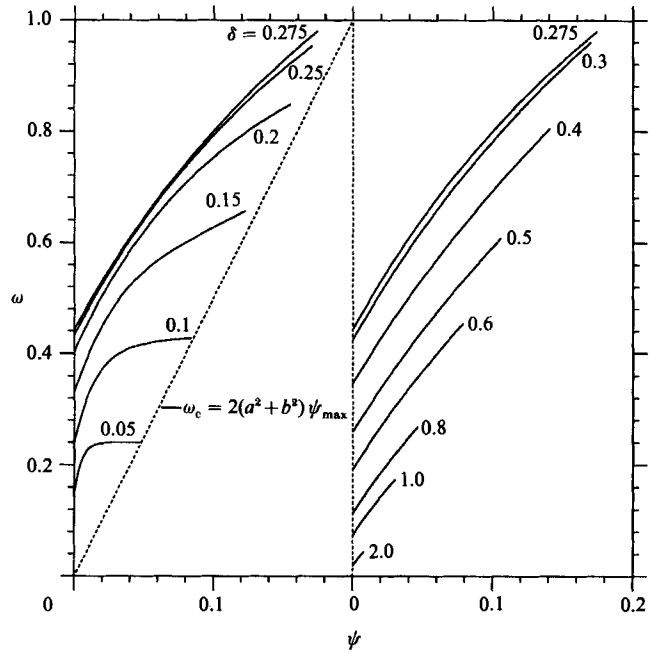

FIGURE 3. $\omega(\psi)$ for $a = 1/b = \sqrt{2}$, a stress-free surface and various δ. Left: $\delta = 0.05$, 0.01, 0.15, 0.2, 0.25, 0.275. Right: $\delta = 0.275$, 0.3, 0.4, 0.5, 0.6, 0.8, 1, 2.

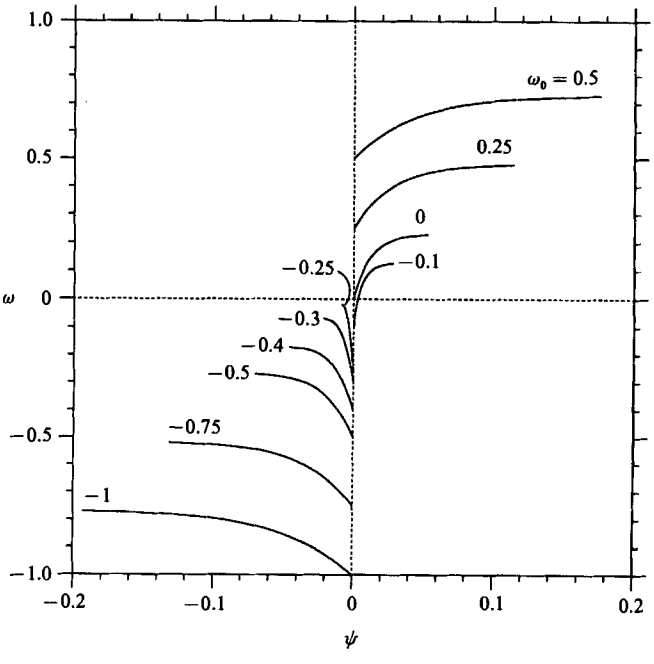

FIGURE 4. $\omega(\psi)$ for $a = 1/b = 1.1$, $\delta = 0.1$ and various ω_0. $\omega_0 = -1$, -0.75, -0.5, -0.4, -0.3, -0.25, -0.1, 0, 0.25, 0.5.

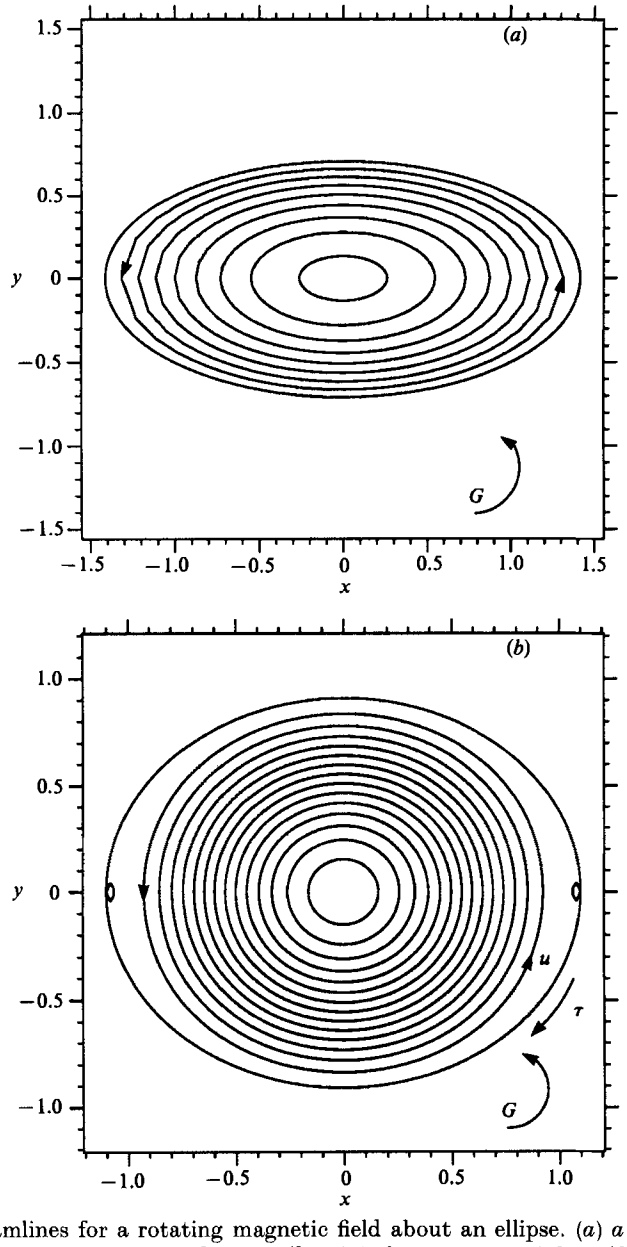

FIGURE 5. Streamlines for a rotating magnetic field about an ellipse. (*a*) $a = 1/b = \sqrt{2}$, $\delta = 0.1$, stress-free surface, no separation. (*b*) $a = 1/b = 1.1$, $\delta \to \infty$, $\omega_0 = -0.2125/\delta^2$. Separation has just occurred at ends of the major axis.

by an appropriate surface stress). Near the opposite limit, however, when δ is large and G is distributed evenly over V, the corresponding range is greater. The localization of the force near the surface may thus be thought of as inhibiting separation and instability of the flow. The solutions plotted in the figure are for values close to this range. The steepening of the gradients as flow reversal is approached (with consequent likelihood of instability) is marked. Another feature of note is the almost linear relationship of the central values of ω and ψ (the endpoints of the curves).

The streamline patterns for these flows tend to be similar in appearance and relatively uninformative. Two cases are drawn in figure 5. For figure 5(*a*) $a/b = 2$, $\delta = 0.1$ and the surface S is stress-free. For this low value of δ, the vorticity is almost constant in the interior of the ellipse, with correspondingly nearly elliptical streamlines. The flow speed, as manifest in the distance between streamlines, is fairly uniform across most of the ellipse, decelerating near the ends of the major axis as one would expect. In figure 5(*b*), however, a more revealing flow is shown for $a = 1/b = 1.1$ in the limit of δ large, with a surface stress acting in opposition to the motion. The magnitude of this stress and the corresponding constant surface vorticity value have been chosen so that separation has just begun near the ends of the major axis. Physically, it comes as no surprise that separation begins near the point of maximum curvature. The velocity is much smaller on the surface than in the main body of fluid, but does not vanish everywhere on S simultaneously as would be required by a solid boundary.

While it is of theoretical interest to consider all values of ω_0, it is clearly important to keep in mind which values are physically likely in any particular problem. Because of its frictional form, the surface stress given by (5.6) can never drive a flow which is everywhere in the opposite sense to G. However for large values of the friction coefficient α (greater than the critical value on figure 5*b*), the flow can separate off from the wall forming small regions where the circulation is opposed to G. In the context of continuous casting, this can lead to inhomogeneities in the solidified product near the surface stagnation points, increasing the likelihood of crack formation. As the metal solidifies, it tends to solidify fastest in the regions of maximum surface curvature. As a result, the departures from circularity of the liquid core diminish, as does the likelihood of separation.

7. Concluding remarks

In this paper we have described a fast method for calculating steady, forced, high-Reynolds-number flows in two dimensions or axisymmetry. In these geometries the vorticity has a functional dependence on the streamfunction which we calculate iteratively. The method may be used inside any region upon whose boundary either the vorticity or the tangential stress is prescribed. It does not, however, apply in general inside slip-free boundaries, when the boundary layer is energetically dominant. As we saw in §3, the weak boundary layer associated with a jump in stress (such as that on a free surface) can be incorporated into the theory. It leads to an $O(\nu)$-correction to the core flow, and thus the results obtained by neglecting it should be reasonably accurate even for moderate Reynolds numbers. In such a boundary layer the vorticity is not constant on streamlines and so the flow cannot be represented by an (ω, ψ)-plot as in figure 3.

It is not necessary for the function $\omega(\psi)$ to be single-valued for the method to be applicable, but this simplifies the process. When it is not, and likewise when the flow consists of two or more disconnected circulatory regions, a modicum of numerical care is required to ensure correct representation of the flow. We see from the curves on the right of figure 3 that in some circumstances the function $\omega(\psi)$ is not only monotonic but indeed nearly linear. This suggests that those flows may be approximated by a linear equation (4.1), with obvious advantages (e.g. Jones *et al.* 1976). One would expect this approximation to be a good one when there is no localization forced upon the flow, that is when the forcing is slowly varying inside a smooth, stress-free surface S.

The method may be applied to a variety of magnetohydrodynamic problems such as the shaping, stirring or levitation of liquid metals. It is particularly well suited for many of these problems, when the free-surface shape S is not known *a priori* and must itself be determined by some iterative technique, with which the method we have described can be merged. Other applications include low-Prandtl-number convection and various oceanographic models. In all these cases, the forcing is independent of the velocity field. However, there is no reason in principle why the iterative procedure should not be used even when the forcing does vary with the flow. How useful the method is in that case naturally depends on the ease with which the forcing for a given flow may be calculated. This greatly widens the scope of possible applications. Any inertially dominated flow problem may be approached using this technique, provided the energy dissipation occurs in the main body of the fluid rather than in some boundary layer.

It is shown in the contiguous paper on stability (Mestel 1989) that the function $\omega(\psi)$ and in particular its derivative are of great significance in determining the stability of the flow. The iterative method, which directly obtains $\omega(\psi)$, is thus well-suited for use in conjunction with the stability analysis of that paper. We find there is a correlation, if not a correspondence, between those flows deemed unstable by the criteria of that paper, and those flows for which the iterative method we have described here behaves delicately. That is to say, for stable flows the method converges rapidly for any initial condition, while for ones close to instability it requires a close initial estimate. This is of course not surprising, as iteration towards a steady state involves processing perturbations about that state, which we might expect to grow if the basic flow is unstable.

While on the subject of stability, it is worth noting that many of the two-dimensional flows we have been studying may be unstable to three-dimensional disturbances. In particular, Bayly (1987) has shown that elliptical Euler flows with constant vorticity are unstable. Now the flows we have been considering (e.g. in figure 5) are of this type very close to their central stagnation points. It is not clear whether the effects of viscosity and rotational forcing may be neglected over the appropriate lengthscale, but if this is the case, such flows will be unstable unless they are locally circular.

In conclusion, I would like to repeat my thanks to Dr Owen Tutty for his help in supplying the reliable Navier–Stokes code against which the method described in this paper was tested. I am also grateful to a referee for some helpful comments.

REFERENCES

ABRAMOWITZ, M. & STEGUN, I. A. 1965 *Handbook of Mathematical Functions*. Dover.

BATCHELOR, G. K. 1956 On steady laminar flow with closed streamlines at large Reynolds number. *J. Fluid Mech.* **1**, 177–190.

BATCHELOR, G. K. 1967 *An Introduction to Fluid Dynamics*. Cambridge University Press.

BAYLY, B. J. 1987 Three-dimensional instability of elliptical flow. *Phys. Rev. Lett.* **57**, 2160–2163.

BUSSE, F. H. & CLEVER, R. M. 1981 An asymptotic model of two-dimensional convection in the limit of low Prandtl number. *J. Fluid Mech.* **102**, 75–83.

DAVIDSON, P. A. & HUNT, J. C. R. 1987 Swirling recirculating flow in a liquid metal column generated by a rotating magnetic field. *J. Fluid Mech.* **185**, 67–106.

ETAY, J. 1980 Formage et guidage des metaux liquides sous l'action de champs magnetiques alternatifs. *Report de D.E.A. de Mécaniques des Fluides, Inst. Natn. Polytechnique, Grenoble.*

FAUTRELLE, Y. R. 1981 Analytical and numerical aspects of the electromagnetic stirring induced by alternating magnetic fields. *J. Fluid Mech.* **102**, 405–430.

JONES, C. A., MOORE, D. R. & WEISS, N. O. 1976 Axisymmetric convection in a cylinder. *J. Fluid Mech.* **73**, 353–388.

MESTEL, A. J. 1982 Magnetic levitation of liquid metals. *J. Fluid Mech.* **117**, 27–43.

MESTEL, A. J. 1984 On the flow in a channel induction furnace. *J. Fluid Mech.* **147**, 431–447.

MESTEL, A. J. 1988 More accurate skin-depth solutions. *Liquid Metal Magnetohydrodynamics. Proc. IUTAM Symp. Riga* 1988. Kluwer.

MESTEL, A. J. 1989 On the stability of high Reynolds number flows with closed streamlines. *J. Fluid Mech.* **200**, 19–38.

MOFFATT, H. K. 1965 On fluid flow induced by a rotating magnetic field. *J. Fluid Mech.* **22**, 521–528.

MOFFATT, H. K. 1984 High frequency excitation of liquid metal systems. *Metallurgical Applications of Magnetohydrodynamics. Proc. IUTAM Symp. Cambridge* 1982. The Metals Society.

READ, P. L., RHINES, P. B. & WHITE, A. A. 1986 Geostrophic scatter diagrams and potential vorticity dynamics. *J. Atmos. Sci.* **43**, 3226–3240.

SHERCLIFF, J. A. 1981 Magnetic shaping of molten metal columns. *Proc. R. Soc. Lond.* A **375**, 455–473.

SNEYD, A. D. 1979 Fluid flow induced by a rapidly alternating or rotating field. *J. Fluid Mech.* **92**, 35–51.

SNEYD, A. D. & MOFFATT, H. K. 1982 The fluid dynamics of the process of levitation melting. *J. Fluid Mech.* **117**, 45–70.

TREFETHEN, L. N. 1986 (Ed.) Special issue on numerical conformal mapping. *J. Comp. Appl. Maths.* **14**, 1 & 2.

TUTTY, O. & PEDLEY, T. J. 1989 Computations of oscillatory flow in a non-uniform channel. (In preparation for *J. Fluid Mech.*)